crystals

MDPI

Article

Crystal Structure and Phase Transition of the C–H···F–H-Bonded Supramolecular Compound with 4-Nitroanilinium Based on 18-Crown-6

Chun-li Zhu, Yang Liu *, Kun Wang, Yuan Chen and Zun-qi Liu *

College of Chemical Engineering, Xinjiang Agricultural University, Urumqi 830052, China; zhuchunlixj90@163.com (C.L.-Z.); xjdgbz2001@163.com (K.W.); chenyuanxj90@163.com (Y.C.)

* Correspondence: liuyangxj85@163.com (Y.L.); lzq@xjau.edu.cn (Z.-Q.L.); Tel.: +86-991-876-2834 (Z.-Q.L.)

Academic Editor: Alberto Girlando

Received: 3 August 2017; Accepted: 7 September 2017; Published: 12 September 2017

Abstract: A novel inorganic-organic hybrid supramolecular macrocyclic compound, (4-nitroanilinium)(18-crown-6)(PF_6)(**1**), was synthesized and characterized by infrared spectroscopy, thermogravimetric analysis, elemental analysis, differential scanning calorimetry (DSC), and single-crystal X-ray diffraction. Crystal **1** is found to comprise 1D C–H···F–P hydrogen-bonded chains of (4-nitroanilinium$^+$)(18-crown-6) supramolecular cations and PF_6^- anions. DSC measurements confirm that **1** undergoes a reversible phase transition at 255 K with a hysteresis width of 6 K. A strong dielectric response is observed above 250 K at a low frequency (500 Hz), suggesting the occurrence of proton transfer in the C–H···F–P hydrogen bonds. A precise analysis on the main packing and structural differences, as well as the changes in the intermolecular interaction between the low- and high-temperature phases, reveals that C–H···F–P hydrogen bonds are the main factors affecting phase transition and dielectric behavior.

Keywords: crystal structure; phase transition; dielectric response; crown ether; C–H···F–P hydrogen bonds

1. Introduction

Research on solid-state materials is increasingly attracting interest owing to their potential versatile technical applications, such as molecular sensors, switches, and data-storage devices [1–4]. Among them, phase-transition crystalline materials are important and often cause significant changes in physical and chemical properties. Various components of phase-transition materials have been investigated, including metal-organic, pure inorganic, organic hydrogen-bonded, and organic-inorganic hybrid materials. Among them, inorganic-organic hybrid complexes exhibit fascinating structures or prominent functionalities because of their hybrid inorganic-organic advantages [5–9]. The crystalline materials of inorganic-organic hybrid compounds with phase-transition or peculiar molecular packing modes display remarkable and unusual dielectric properties, ferroelectric transfer, superconductivity, and magnetic coupling [10–13].

Ammonium-crown ether-based supramolecular assemblies in inorganic-organic compounds have been extensively investigated and occupy a special position [14–16]. The reason is that the size of the crown ether and the nature of the ammonium cation (NH_4^+, RNH_3^+, and $R_2NH_2^+$) can influence the stability of the host–guest complexes. A common structural feature of these complexes is that the $-NH_3^+$ head is tightly anchored into the cavity of the crown ether [16,17]. Supramolecular assemblies can be obtained through multiform weak intermolecular interactions, such as hydrogen bonds, charge transfer, and van der Waals forces. For example, supramolecular structures can afford multiple N–H···O strong H-bonds, thereby contributing to dielectric or ferroelectric behaviors. The hydrogen

bonds of such structures are weaker than other chemical bonds, such as covalent bonds [18,19]. During temperature changes, the hybrid crystalline materials constructed by hydrogen bonds can easily undergo transformations, thereby leading to phase transition. Xiong et al. reported a novel mononuclear metal–organic compound, [Cu(Hdabco)(H_2O)Cl_3], which forms a 3D network by N–H···O and O–H···O hydrogen bond interactions. The crystal displays a paraelectric-to-ferroelectric phase transition triggered by the motion of the anions or cations and proton transfer of the hydrogen bonds [20–22]. Intermolecular hydrogen bonds also play an important role in the stabilization of the structure. In most cases, the most widely used hydrogen bond patterns are C–H···O, N–H···O, and O–H···O. By contrast, other heteroatoms with high negativity (e.g., fluorine) functioning as proton acceptors have rarely been explored and compared with oxygen or nitrogen atoms. Although fluorine ion acts as a strong proton acceptor, covalently bound fluorine is a weak intermolecular hydrogen bond acceptor [23,24].

Preparing suitable materials with variable-temperature dielectric response, especially in relatively high- and low-frequency range, is useful for the identification of phase-transition materials. Pure inorganic compounds are well developed, but supramolecular compounds that possess preponderant inorganic and organic properties as phase transition materials are difficult to prepare [25,26]. Previously, we reported an organic–inorganic hybrid supramolecular compound, [(4-nitroanilinium)(18-crown-6)][BF_4](CH_3CN), which displays a 1D supramolecular chain structure by weak hydrogen bonds between the $-NH_3^+$ moieties and $-NO_2$ of adjacent 4-nitroanilinium interaction through the cavity of 18-crown-6 molecule [27]. The dielectric response of the crystal correlates with the direction of hydrogen bonds, suggesting the occurrence of proton transfer in the hydrogen bonds. In the current study, an inorganic-organic hybrid phase-transition material, (4-nitroanilinium)(18-crown-6)(PF_6) (**1**), was synthesized and characterized. The crystal forms a 1D chain structure via C–H···F–P hydrogen bonds. The differential scanning calorimetry (DSC), single-crystal X-ray diffraction data, and dielectric constant measurements indicate that **1** undergoes a reversible phase transition from high-temperature (HT) phase to low-temperature (LT) phase with the same space group $P2_1/c$. The driving force of the phase transition mainly originates from the proton transfer in C–H···F–P hydrogen bonds.

2. Results and Discussion

2.1. Spectral Properties

The structure of **1** was confirmed by IR spectra (Figure S1). The IR spectra of **1** show a strong broad band from 3305 cm^{-1} to 2655 cm^{-1}, indicating that the $-NH_2$ group is protonated by means of intermolecular N–H···O hydrogen bonds. A series of characteristic peaks at 1597, 1554, 1527, 1496, and 1352 cm^{-1}, are assigned to the skeletal vibrations of the aromatic rings. The bands within the 993–754 cm^{-1} range are characteristic peaks of the stretching vibrations of P–F bond of the PF_6^- anion. The characteristic peaks of 18-crown-6 molecules are observed at 1099, 964, 840, and 740 cm^{-1}, and these regions are attributed to the specific –O–C–C– structural unit. IR spectra analysis shows the existence of three effective constituents in **1**.

2.2. DSC and TG Analysis

DSC can be used to determine the reversible phase transition of a compound triggered by temperature and detect the existence of heat anomaly during heating and cooling procedures. When the compound undergoes a phase transition with thermal entropy change, reversible heat anomalies can be detected. In the DSC spectrum of the present study, no sharp peaks are observed but observable inflexion points (i.e., an endothermic peak at 258 K upon heating and an exothermic peak at 252 K upon cooling) are found (Figure 1). These observed heat anomalies represent a reversible phase transition with a 6 K hysteresis. Nearly no hysteresis and small heat anomalies reveal the continuous characteristic of the phase transition, effectively indicating a second-order phase transition.

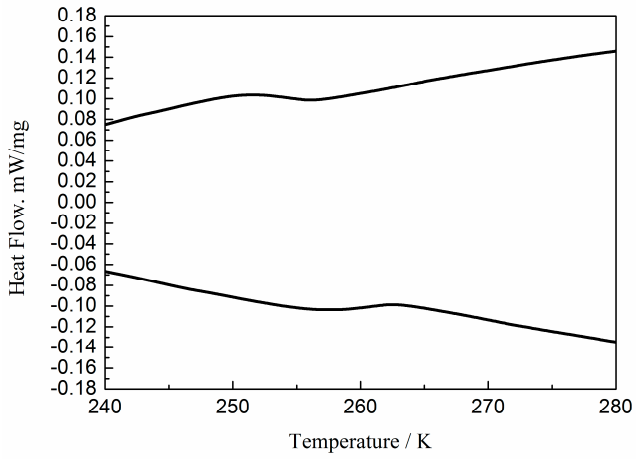

Figure 1. DSC curves for compound **1** in terms of reversible phase transitions.

The thermal behaviors of **1** are discussed in detail through thermogravimetric analysis (TG) and differential thermal analysis (DTA) measurements from 300 K to 850 K (Figure S2). The DTA curve shows a sharp endothermic peak at 433.5 K, and this peak corresponds to the melting point of **1**. The relevant TG curve reveals three main regions of weight loss. The structure of **1** remains undecomposed up to 433.5 K. The first starts with the weight loss of approximately 44.53%, indicating the escape of the 18-crown-6 molecule (calcd. at 42.53%). The second weight loss is observed in the range of 520.6–761.4 K, amounting to nearly 23.49% weight loss. This condition indicates the decomposition of the 4-nitroanilinium cation. The third step is the loss of the two PF_6^- anions and one HPF_6 molecule, showing a weight loss of 31.98% (35.08% theoretically).

2.3. Description of Crystal Structure

To fully understand the details of the phase transition, the structures of **1** were determined at LT (100 K) and HT (296 K). Crystallographic data and details of collection and refinement are listed in Table 1. At LT, the crystals are in the space group $P2_1/c$, with cell parameters a = 10.9077(9) Å, b = 23.296(2) Å, c = 21.5573(15) Å, and β = 113.2773°. The HT phase structure determined at 296 K is also monoclinic $P2_1/c$ with axis lengths similar to those in the LT phase, but shows modest changes in the length of the b and c axes (b = 23.778(6) Å, c = 21.933(5) Å) and same-degree change in the β angle (β = 113.678(10)°). Therefore, **1** underwent isosymmetric structural phase transition. The structural parameters of **1** have very small change at different temperatures, indicating that the phase transitions may be caused by other factors, such as proton transfer and the change of molecular thermal energy.

Table 1. Crystallographic data for compound **1**.

Temperature	100 K	296 K
Chemical formula	$C_{36}H_{62}F_{12}N_4O_{16}P_2$	$C_{36}H_{62}F_{12}N_4O_{16}P_2$
Formula weight	1096.8230	1096.8230
Crystal size (mm^3)	0.21 × 0.2 × 0.19	0.21 × 0.20 × 0.19
Crystal system	monoclinic	monoclinic
Space group	$P2_1/c$	$P2_1/c$
a (Å)	10.9077(9)	11.067(3)
b (Å)	23.296(2)	23.778(6)
c (Å)	21.5573(15)	21.933(5)
α (°)	90.00	90.00
β (°)	113.277(3)	113.678(10)
γ (°)	90.00	90.00
V ($Å^3$)	5032.0(7)	5286(2)

Table 1. *Cont.*

Z	2	2
D_{calc} (g·cm^{-1})	1.448	1.378
$F(000)$	2288.0	2288.0
μ (mm^{-1})	0.198	0.188
Measured 2θ range (°)	0.997/25.010	0.998/25.010
R_{int}	0.0954	0.0797
R ($I > 2\sigma(I)$) [a]	0.1205	0.1606
$_{W}R$ (all data) [b]	0.2093	0.1899
GOF	1.037	1.077

[a] : $R = \sum(|F_o| - |F_c|)/\sum|F_a|$ [b] : $R_W^2 = \sum_w (F_o^2 - F_c^2)^2 / \sum_w (F_o^2)^2$.

The asymmetric unit in LT and HT forms involves two 18-crown-6 molecules, two 4-nitroanilinium cations, one PF_6^- anion, and two half PF_6^- anions (Figure 2). The 4-nitroanilinium cation interacts with 18-crown-6 via six N–H···O hydrogen bonds, thereby forming two similar supermolecular cations: (4-nitroanilinium$^+$)(18-crown-6)(A) (contain N_1 and N_2 atoms) and (4-nitroanilinium$^+$)(18-crown-6)(B) (containing N_3 and N_4 atoms). In supramolecule A, the aromatic ring of 4-nitroanilinium cation is nearly perpendicular to the crown ether plane with dihedral angles of 94.86° (LT) and 93.88° (HT). Apparently, the 18-crown-6 rings are similar to the ideal crown formations D_{3d}, with all O–C–C–O torsion angles being gauche and alternating in sign, and all C–O–C–C torsion angles being *trans*. The ether O atoms are nearly coplanar; O_{10}, O_{12}, and O_{14} are located above the mean O-atom plane and O_9, O_{11}, and O_{13} below the plane. The N_1 atom of the 4-nitroanilinium cation is located in the perching position rather than the nesting position, 0.9023 Å (LT) and 0.8915 Å (HT) higher from the best plane of the six oxygen atoms of the crown ring. The $-NH_3^+$ (N_1) moiety interacts with the six oxygen atoms of 18-crown-6 via three short, approximately linear, N–H···O hydrogen bonds and three long, weak interactions (Figure 2 and Table 2). In the LT structure, the distances between N_1 atoms and O_{10}, O_{12}, and O_{14} in crown ether are 2.8629(8), 2.7849(10), and 2.8308(10) Å, respectively. The distances are shorter than those of the three other O atoms (2.9409(10), 2.9768(9), and 2.9289(9) Å from N_1 to O_9, O_{11}, and O_{13}, respectively). In addition, the bond lengths of N–H···O in the HT structure are slightly longer than those in the LT structure. The results of hydrogen bond analysis for LT and HT structures suggest that the proton presents no distinct transfer in the N–H···O hydrogen bonds of supramolecule A. The finding is similar to that in our previous reported 18-crown-6 clathrates [27].

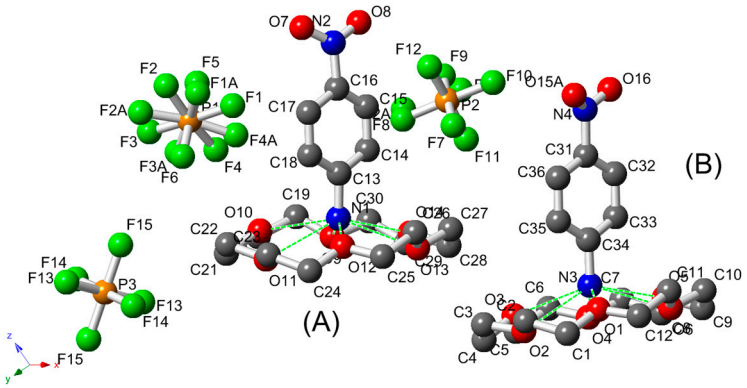

Figure 2. (**A**,**B**) Asymmetric unit of compound **1**.

Table 2. Hydrogen bond N–H···O geometry (Å, °) for complex **1**.

D-H···A	d(D–H)	d(H···A)	d(D···A)	∠DHA
		100 K		
N1–H1WC···O9	0.8268(5)	2.4418(8)	2.9409(10)	119.759(4)
N1–H1WC···O10	0.8268(5)	2.0648(7)	2.8629(8)	161.909(4)
N1–H1WB···O11	0.8239(6)	2.5817(7)	2.9768(9)	110.866(5)
N1–H1WB···O12	0.8239(6)	2.0148(8)	2.7849(10)	115.569(6)
N1–H1WA···O13	0.8209(6)	2.6928(7)	2.9289(9)	98.478(6)
N1–H1WA···O14	0.8209(6)	2.0289(8)	2.8308(10)	165.429(7)
N3–H3WA···O1	0.8228(5)	2.0348(9)	2.8518(2)	172.059(7)
N3–H3WA···O2	0.8228(5)	2.5728(10)	2.9829(9)	112.168(9)
N3–H3WB···O3	0.8228(9)	2.0829(1)	2.9049(2)	175.079(9)
N3–H3WB···O4	0.8228(9)	2.6228(7)	2.9537(7)	105.709(4)
N3–H3WC···O5	0.8218(4)	2.0838(10)	2.8979(3)	170.569(7)
N3–H3WC···O6	0.8218(4)	2.6148(5)	2.9107(8)	102.879(8)
		296 K		
N1–H1WA···O9	0.8895(6)	1.9858(8)	2.8549(3)	165.028(9)
N1–H1WB···O10	0.8889(6)	2.4589(3)	2.9349(10)	113.959(9)
N1–H1WB···O11	0.8889(6)	1.9448(6)	2.8127(9)	165.195(8)
N1–H1WC···O12	0.8886(8)	2.4569(6)	2.9736(9)	117.547(4)
N1–H1WC···O13	0.8886(8)	2.0076(4)	2.8726(8)	164.038(6)
N1–H1WA···O14	0.8895(6)	2.4437(5)	2.9347(7)	115.187(5)
N3–H3WA···O1	0.8886(7)	2.0443(10)	2.9106(8)	164.398(6)
N3–H3WC···O2	0.8886(7)	2.4427(9)	2.9219(4)	114.148(7)
N3–H3WC···O3	0.8886(7)	1.9948(5)	2.8676(7)	166.616(6)
N3–H3WB···O4	0.8887(5)	2.4958(4)	2.9907(10)	115.618(6)
N3–H3WB···O5	0.8887(5)	2.0518(6)	2.9307(8)	169.146(8)
N3–H3WA···O6	0.8886(7)	2.4429(4)	2.9658(5)	117.919(7)

In supramolecule B, the 18-crown-6 ring employs a typical crown formation with a corresponding dihedral angle between the aromatic ring of 4-nitroanilinium cation and the crown ether planes of 93.36° (LT) and 93.38° (HT), which are similar to the corresponding values of 94.86° (LT) and 93.88° (HT) in supramolecule A. The N_3 atom of the $–NH_3^+$ group remains in the perching position, located 0.9087 Å (LT) and 0.8891 Å (HT) from the plane of the oxygen of the crown ring. The hydrogen bond interactions among the nitrogen and oxygen atoms with bond length of N···O are 2.8518(2)–2.9829(9) Å at LT and 2.8676(7)–2.9907(10) Å at HT, respectively. The intermolecular N–H···O hydrogen bond distances are within the usual range. No obvious intermolecular interaction (e.g., π–π interaction) is found between supramolecules A and B. The arrangements of supramolecules A and B are shown in Figure 3; these supramolecules are stacked alternately along the *a*-axis. Furthermore, two PF_6^-anions are presented as counter-ions to the supramolecular cation (4-nitroanilinium$^+$)(18-crown-6). One PF_6^-(P_1) remains disordered over two staggered orientations with a common F_5-P_1-F_6 linear bond in the LT and HT structures. This linear bond is a rotation axis between two stable orientations at a 45° rotational angle. The other PF_6^-(P_2) anion becomes ordered, containing an inversion center near the PF_6^-(P_2) anions (Figure 3S). The F···F distance of common compounds was usually in the range of 2.5–3.2 Å. However, the relatively short F···F bonding distance was 1.46 Å in **1**. This phenomenon may be caused by the inversion center and the tight arrangement of anions and cations.

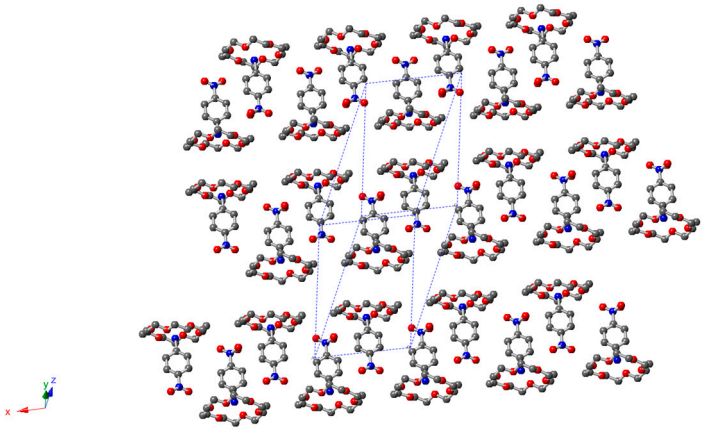

Figure 3. Packing of supramolecular cation (4-nitroanilinium)(18-crown-6) view along the *a* axis.

The phase transition should be accurately examined to discover the important packing and structural differences, as well as the changes in intermolecular interactions. The most effective interactions in **1** are observed as C–H···F–P hydrogen bonds via adjacent 4-nitroanilinium cations and PF_6^- anions. In Figure 4, C–H···F–P hydrogen bonds form two crystallographically-independent 1D chains along *a*-axis at LT and HT (chain A: 4-nitroanilinium contain N_1 and N_2 atoms, PF_6^- anion contains P_1 atom; chain B: 4-nitroanilinium contain N_3 and N_4 atoms, PF_6^- anion contains P_2 atom). In chain A, the C–H···F–P hydrogen bonds between the donor of the 4-nitroanilinium cation (C_{14}, C_{15}, C_{17}, and C_{18}) and acceptor atoms of PF_6^- (F_6, F_2, F_4) anion exhibit bond distances of 3.390–3.499 Å for HT of **1**. In the LT structure, the hydrogen bond interaction strengthens with the distance of C–H···F–P ranging from 3.228 to 3.371 Å. In chain B, the 4-nitroanilinium cation and the PF_6^- anion also relate with each other via intermolecular interaction, while each of them acts as a donor and an acceptor simultaneously. The C–H···F–P bond distance noticeably changes at LT and HT (Table S1). On the basis of the neighboring PF_6^- anions, the shortest P–P bond distances are 10.908 and 11.067 Å in chains A and B at LT and HT, respectively. This finding indicates that as temperature decreases, PF_6^- anions change their position and thus form a short chain in LT. H proton also transfers easily between C atom and F atom in the two chains along the c-axis from LT to HT. The molecular C–H···F–P hydrogen bond interactions play a crucial role in the phase transition with the increase in temperature. In Figure 5, two 1D chains are alternately stacked together to build a supramolecular self-assembly structure in the *b* + *c* plane.

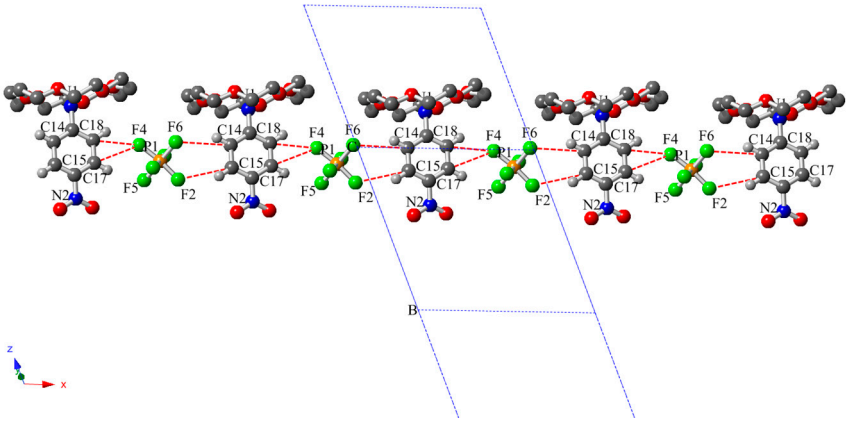

(**A**)

Figure 4. *Cont.*

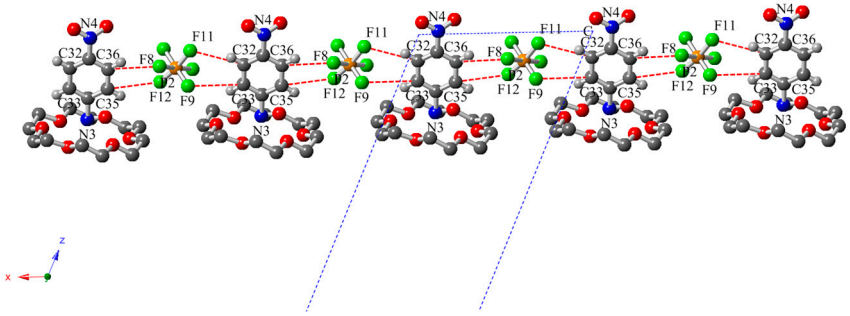

(**B**)

Figure 4. Two kinds of 1D chain molecular structure (**A**,**B**) between fluorine atom of the PF_6^- anion and the adjacent 4-nitroanilinium cation in compound **1** with C–H···F–P hydrogen bond interactions.

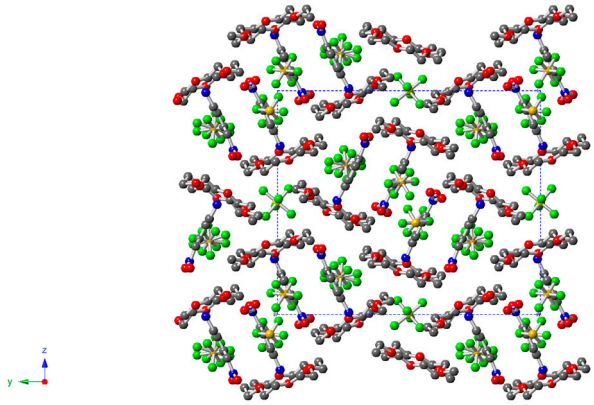

Figure 5. Self-assembly packing of the supramolecular cation and anion along the *a*-axis in compound **1**.

2.4. Dielectric Properties

The variable-temperature dielectric response was measured to further investigate the phase transition in **1**. In the phase transition point, the dielectric permittivity generally shows changes or noticeable anomalies. Given the difficulty in obtaining large crystals, the pressed-powder pellet of **1** was used in dielectric measurements. The temperature dependence of dielectric constant (ε) taken from 100 K to 290 K at 500 Hz to 1 MHz as shown in Figure 6. The graph shows that the frequency increases with the decrease in dielectric constant. The dielectric constant (ε) of **1** reaches its maximum value at 500 Hz, whereas the value directly drops to approximately 2.0 at 1 MHz. At low frequencies, the high dielectric constant value is attributed to space charge polarization. Meanwhile, the dipole reversal of space charge polarization cannot keep up with the alternating current field reversal in the high frequencies. Consequently, the dielectric constant (ε) values gradually decrease with the increase in frequency increasing and remain unchanged at high frequencies. The significant increases in dielectric constant for compound **1** above 250 K can be attributed to inorganic-organic supramolecular structural interactions, which allow proton transfers between intermolecular C–H···F–P hydrogen bonds. This result is consistent with the DSC measurements. From the crystal structure of compound 1 at LT and HT, the intermolecular C–H···F–P hydrogen bond interactions may be the driving force of the phase transition and dielectric behavior.

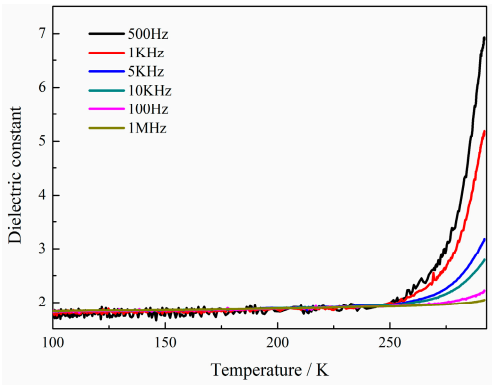

Figure 6. Dielectric constants of compound **1** from 100 K to 300 K at 500 Hz–1 MHz.

3. Experimental

3.1. Material and Instruments

All the reagents and solvents were commercially available and used as received without further purification. Infrared spectra (IR) were recorded on an Affinity-1 spectrophotometer (Shimadzu, Japan) (400–4000 cm^{-1}) Elemental analyses were performed using a Vario EL Elementar Analysensysteme GmbH (Hanau, Germany) in the Collaboration Center of TRW Research, YanZhou, Shandong. Two thermal analyses, TG and DTA, were performed on a TA Q50 instrument (New Castle, DE, USA) under a flowing nitrogen atmosphere with a heating rate of 10 K/min. The heating rate of samples was 10 K min^{-1}. DSC measurements were performed on a TA Q2000 DSC (TA Instruments, Inc., New Castle, DE, USA) instrument from 240 K to 280 K, and the heating rate was 10 K min^{-1} at nitrogen atmosphere pressure. Dielectric constants of the crystal material were conducted using a TH2828 Precision LCR meter (Changzhou Tonghui Electronic Co., Ltd., Changzhou, China) within the frequency range of 500 Hz–1 MHz. The approximate temperature range was from 100 K to 290 K with an applied electric field of 1.0 V.

3.2. Preparation of (4-Nitroanilinium)(18-Crown-6)(PF_6) (**1**)

Through the slow evaporation of a mixed solution containing 45% hexafluorophosphate acid (70 mg), 4-nitroaniline (20 mg), and 18-crown-6 (200 mg) in methanol (50 mL) (Scheme 1), we obtained **1**. Several days later, transparent yellow block crystals were collected in ca. 85% yield. The chemical formulas of **1** were determined using elemental analysis and X-ray crystallographic analyses. Given anal. calcd. for $C_{36}H_{62}F_{12}N_4O_{16}P_2$: C, 39.42%; H, 5.70%; N, 5.11%, the results were C, 39.36%; H, 5.59%; N, 5.03%.

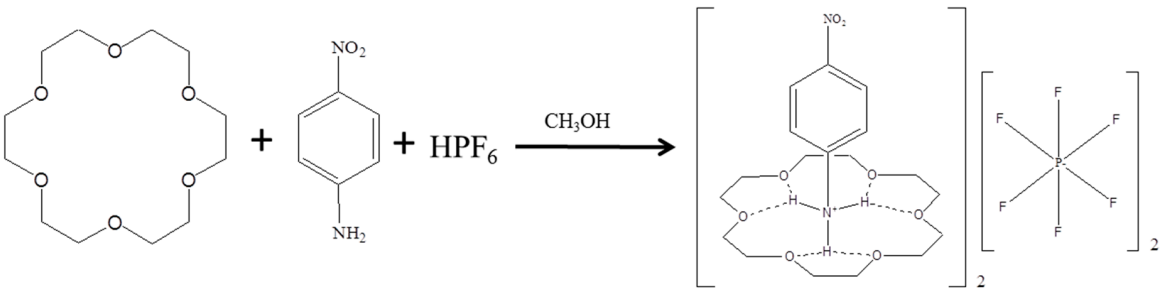

Scheme 1. Synthesis of compound **1**.

3.3. Crystal Structure Determination

Single-crystal data of **1** were collected at 100 and 296 K on a Bruker AXS CCD acre-detector diffractometer (Karlsruhe, Germany)with graphite-monochromated MoKα radiation (λ = 0.71073 Å). The structure of **1** was determined using direct methods and successive Fourier synthesis and then refined by full-matrix least-squares method on F^2 using the SHELXL-2014 software package. The parameters were refined using anisotropic temperature factors. Hydrogen atoms bonded to the carbon and nitrogen atoms were placed in the calculated position and refined as a riding mode with a fixed C–H bond distance of 0.95 Å. The crystallographic data for **1** at 100 and 296 K are summarized in Table 1.

CCDC-1541783 (100 K) and -1541784 (296 K) contains the supplementary crystallographic data for this paper. These data can be obtained free of charge from The Cambridge Crystallographic Data Center via www.ccdc.cam.ac.uk/data_request/cif.

4. Conclusions

The inorganic-organic hybrid supramolecular macrocyclic **1** was synthesized and structurally characterized. In this structure, supramolecular cationic structures are formed via N–H···O hydrogen bond interactions between 4-nitroanilinium and 18-crown-6. The supramolecular cations and inorganic anions are arranged alternately and linked to 1D chain via C–H···F–P hydrogen bonds along the *a*-axis. The combined DSC, dielectric measurement, and variable-temperature structural analysis reveal that **1** is an isostructural phase transition material and undergoes phase transition at 255 K. The dielectric response of the crystal increases from 100 K to 290 K within the measurement-frequency range of 500 Hz to 1 MHz with the outer electric field. This characteristic may be attributed to the occurrence of proton transfers between intermolecular C–H···F–P hydrogen bonds. The said observations indicate that intermolecular interactions (C–H···F–P hydrogen bonds) are the main factor to drive the phase transition and dielectric behavior.

Supplementary Materials: The following are available online at www.mdpi.com/2073-4352/7/9/276/s1, Figure S1: IR spectrum of compound **1**; Figure S2: TG and DTA curves for compound **1**; Figure S3: Molecular graph of a model hexafluorophosphate dimer in configuration; Table S1: Hydrogen-bond C–H···F–P geometry (Å, °) for complex **1**; Table S2: Selected bond distances and angles for compound 1 (Å, °).

Acknowledgments: The present work was supported by the National Natural Science Foundation of China (no. 21561030), Program for High-Level Talents Introduction of the Xinjiang Uygur Autonomous Region and the "1000 Talent Plan" on Overseas High-Level Talents Introduction (CCCPC).

Author Contributions: Zun-qi Liu designed the method and wrote the manuscript; Yuan Chen synthesized the crystalline materials. Yang Liu and Kun Wang supported the dielectric constant and DSC measurements. Chun-Li Zhu analyzed the crystal data of **1**. All authors have given approval the final version of the paper.

Conflicts of Interest: The authors declare no conflict of interest.

References

1. Horiuchi, S.; Ishii, F.; Kumai, R.; Okimoto, Y.; Tachibana, H.; Nagaosa, N.; Tokura, Y. Ferroelectricity near room temperature in co-crystals of nonpolar organic molecules. *Nat. Mater.* **2005**, *4*, 163–166. [CrossRef] [PubMed]
2. Akutagawa, T.; Koshinaka, H.; Sato, D.; Takeda, S.; Noro, S.I.; Takahashi, H.; Kumai, R.; Tokura, Y.; Nakamura, T. Ferroelectricity and polarity control in solid-state flip-flop supramolecular rotators. *Nat. Mater.* **2009**, *8*, 342–347. [CrossRef] [PubMed]
3. Xie, Y.R.; Zhao, H.; Wang, X.S.; Qu, Z.R.; Xiong, R.G.; Xue, X.; Xue, Z.L.; You, X.Z. 2D Chiral Uranyl(v1) coordination polymers with second-Harmonic Generation Response and Ferroelectric Properties. *Eur. J. Inorg. Chem.* **2003**, *2003*, 3712–3715. [CrossRef]
4. Ye, H.Y.; Ge, J.Z.; Tang, Y.Y.; Li, P.F.; Zhang, Y.; You, Y.M.; Xiong, R.G. Molecular Ferroelectric with Most Equivalent Polarization Directions Induced by the Plastic Phase Transition. *J. Am. Chem. Soc.* **2016**, *138*, 13175–13178. [CrossRef] [PubMed]

5. Sun, Z.H.; Chen, T.; Luo, J.H.; Hong, M.C. Bis(imidazolium) L-Tartrate: A Hydrogen-Bonded Displacive-Type Molecular Ferroelectric Material. *Angew. Chem. Int. Ed.* **2012**, *51*, 3871–3876. [CrossRef] [PubMed]
6. Liu, Z.Q.; Kubo, K.; Noro, S.I.; Akutagawa, T.; Nakamura, T. Design of Crystalline Speces for Molecular Rotations in Crystals. *Cryst. Growth Des.* **2014**, *14*, 537–543. [CrossRef]
7. Hoshino, N.; Yoshii, Y.; Aonuma, M.; Kubo, K.; Nakamura, T.; Akutagawa, T. Supramolecular Rotators of (Aniliniums)(18-crown-6) in Electrically Conductin [Ni(dmit)2] Crystals. *Inorg. Chem.* **2012**, *51*, 12968–12975. [CrossRef] [PubMed]
8. Tang, Y.Z.; Gu, Z.F.; Xiong, J.B.; Gao, J.X.; Liu, Y.; Wang, B.; Tan, Y.H. Unusual sequential reversible phase transitions containing switchable dielectric behaviors in cyclopentyl ammonium 18-crown-6 perchlorate. *Chem. Mater.* **2016**, *28*, 4476–4482. [CrossRef]
9. Liu, Z.-Q.; Liu, Y.; Wang, J.F.; Yang, G.F. A novel proton transfer supramolecular compound induced by N–H-O hydrogen bond through 18-crown-6: Syntheses structure, and dielectric properties. *Inorg. Chem. Commun.* **2015**, *61*, 109–112. [CrossRef]
10. Fu, D.W.; Dai, J.; Ge, J.Z.; Ye, H.Y.; Zhang, Y. Synthesis, structure and dielectric properties of the 2D K-tetrazole complex $[K_2(4\text{-TPA})_2(H_2O)_2]$n. *Inorg. Chim. Acta* **2010**, *363*, 2584–2589. [CrossRef]
11. Modec, B. The Solid state structure of pyridinium hydrogen squarate. *J. Mol. Struct.* **2015**, *1099*, 54–57. [CrossRef]
12. Zhang, T.; Chen, L.Z.; Gou, M.; Li, Y.H.; Fu, D.W.; Xiong, R.G. Ferroelectric Homochiral Organic Molecular Crystals. *Cryst. Growth Des.* **2010**, *10*, 1025–1027. [CrossRef]
13. Shi, C.; Zhang, X.; Cai, Y.; Yao, Y.F.; Zhang, W. A chemically triggered and thermally switched dielectric constant transition in a metal cyanide based crystal. *Angew. Chem. Int. Ed.* **2015**, *54*, 6206–6210. [CrossRef] [PubMed]
14. Tang, Y.Z.; Yu, Y.M.; Xiong, J.B.; Tan, Y.H.; Wen, H.R. Unusual high-temperature reversible phase transition behavior structure and dielectric ferroelectric properties of two new crown ether clathrates. *J. Am. Chem. Soc.* **2015**, *137*, 13345–13351. [CrossRef] [PubMed]
15. Li, Q.; Shi, P.-P.; Ye, Q.; Wang, H.-T.; Wu, D.H.; Ye, H.Y.; Fu, D.W.; Zhang, Y. A switchable molecular dielectric with two sequential reversible phase transition: $[(CH_3)_4P]_4[Mn(SCN)_6]$. *Inorg. Chem.* **2015**, *54*, 10642–10647. [CrossRef] [PubMed]
16. Nishihara, S.; Ren, X.M.; Akutagawa, T.; Nakamura, T. Crystal structure and magnetic properties of $[Ni(dmit)_2]$ salts including (4-fluoroanilinium)([18]crown-6) and (4-methylanilinium)([18]crown-6) supramolecular cations. *Polyhedron* **2005**, *24*, 2844–2848. [CrossRef]
17. Ohshima, Y.; Kubo, K.; Matsumoto, T.; Ye, H.Y.; Noro, S.I.; Akutagawa, T.; Nakamura, T. One-dimensional supramolecular columnar structure of trans-syn-trans-dicyclohexano[18]crown-6 and organic ammonium cations. *CrystEngComm* **2016**, *18*, 7959–7964. [CrossRef]
18. Ge, J.Z.; Fu, X.Q.; Hang, T.; Ye, Q.; Xiong, R.G. Reversible phase transiton of the 1:1: Complexes of 18-crown-6 with 4-ethoxyanilinium perchlorate. *Cryst. Growth Des.* **2010**, *10*, 3632–3637. [CrossRef]
19. Morimoto, M.; Irie, M. Photochemical control of dielectric peroperties based on intermolecular proton transfer in a hydrogen bonded diarylethene crystal. *Chem. Commun.* **2011**, *47*, 4186–4188. [CrossRef] [PubMed]
20. Ye, Q.; Shi, P.-P.; Chen, Z.Q.; Akutagawa, T.; Noro, S.-I.; akamura, T. Flexible *cis*-cyclohexane-1,4-diammonium ion in magnetic $[Ni(dmit)_2]$ crystals. *Eur. J. Inorg. Chem.* **2012**, *2012*, 3732–3739. [CrossRef]
21. Zhang, Y.; Zhang, W.; Li, S.H.; Ye, Q.; Cai, H.L.; Deng, F.; Xiong, R.G.; Huang, S.D. Ferroelectricity induced by ordering of twisting motion in a molecular rotor. *J. Am. Chem. Soc.* **2012**, *134*, 11044–11049. [CrossRef] [PubMed]
22. Wei, Y.; Zhu, Y.; Song, Y.L.; Hou, H.W.; Fan, Y.T. A novel inorganic organic tetragonal prism supramolecular compound [Fe(NCS)][(Hbpy)(Hbpy)(bpy)]: Crystal structure and non-linear optical properties. *Inorg. Chem. Commun.* **2002**, *5*, 166–170. [CrossRef]
23. Jin, Y.; Yu, C.-H.; Wang, Y.-F.; Li, S.-C.; Zhang, W. synthesis and structural phase transitions of copper(II) and iron(III) complexes containing $[(C_8H_{12}NO)(18\text{-crown-6})]^+$ supramolecular cations. *Z. Anorg. Allg. Chem.* **2014**, *640*, 1499–1505. [CrossRef]
24. Ye, H.Y.; Cai, H.L.; Ge, J.Z.; Xiong, R.-G. Reversible structural phase transiton of pyridinium 4-carboxylic acid perchlorate. *J. Appl. Cryst.* **2010**, *43*, 1031–1035. [CrossRef]

25. Han, X.B.; Hu, P.; Shi, C.; Zhang, W. Structure phase transitions and dielectric transitions in a1,4-diazabicyclo[2,2,2]octane (dabco) based organic crystal. *J. Mol. Struct.* **2017**, *1127*, 372–376. [CrossRef]
26. Junk, P.C.; Raston, C.L. Hydrolytic stability of $SnCl_4$ and $GaCl_3$ in the formation of [cis-$SnCl_4(H_2O)_2$] 18-crown-6 $2H_2O$ and [2,2,2]cryptand $+2H^+$][$GaCl_4$]. *Inorg. Chim. Acta* **2004**, *357*, 595–599. [CrossRef]
27. Liu, Z.Q.; Liu, Y.; Chen, Y.; Zhao, W.-Q.; Fang, W.-N. Synthesis, characterization, and phase transition of an inorganic-organic hybrid compound, [(3-nitroanilinium)(18-crown-6)] [IO_4-](CH_3OH). *Chin. Chem. Lett.* **2017**, *28*, 297–301. [CrossRef]